



Politecnico di Torino

Porto Institutional Repository

[Article] Engineering the strain field for the control of quantum confinement:
An analytical model for arbitrary shape nanostructures

Original Citation:

Mazzer M., De Giorgi M., Cingolani R., Porello G., Rossi F., Molinari E. (1998). *Engineering the strain field for the control of quantum confinement: An analytical model for arbitrary shape nanostructures*. In: [JOURNAL OF APPLIED PHYSICS](#), vol. 84 n. 7, pp. 3437-3441. - ISSN 0021-8979

Availability:

This version is available at : <http://porto.polito.it/2498484/> since: July 2012

Publisher:

AIP

Published version:

DOI:[10.1063/1.368517](https://doi.org/10.1063/1.368517)

Terms of use:

This article is made available under terms and conditions applicable to Open Access Policy Article ("Public - All rights reserved") , as described at http://porto.polito.it/terms_and_conditions.html

Porto, the institutional repository of the Politecnico di Torino, is provided by the University Library and the IT-Services. The aim is to enable open access to all the world. Please [share with us](#) how this access benefits you. Your story matters.

Publisher copyright claim:

Copyright 1998 American Institute of Physics. This article may be downloaded for personal use only. Any other use requires prior permission of the author and the American Institute of Physics. The following article appeared in "[JOURNAL OF APPLIED PHYSICS](#)" and may be found at [10.1063/1.368517](https://doi.org/10.1063/1.368517).

(Article begins on next page)

Engineering the strain field for the control of quantum confinement: An analytical model for arbitrary shape nanostructures

M. Mazzer, M. De Giorgi, R. Cingolani, G. Porello, F. Rossi et al.

Citation: *J. Appl. Phys.* **84**, 3437 (1998); doi: 10.1063/1.368517

View online: <http://dx.doi.org/10.1063/1.368517>

View Table of Contents: <http://jap.aip.org/resource/1/JAPIAU/v84/i7>

Published by the [American Institute of Physics](#).

Related Articles

Determination of conduction band offset between strained CdSe and ZnSe layers using deep level transient spectroscopy

Appl. Phys. Lett. **100**, 252110 (2012)

Electronic band gaps and transport in aperiodic graphene superlattices of Thue-Morse sequence

Appl. Phys. Lett. **100**, 252402 (2012)

Influence of linearly polarized radiation on magnetoresistance in irradiated two-dimensional electron systems

Appl. Phys. Lett. **100**, 242103 (2012)

Laterally confined two-dimensional electron gases in self-patterned LaAlO₃/SrTiO₃ interfaces

Appl. Phys. Lett. **100**, 231607 (2012)

Monte Carlo studies of the intrinsic time-domain response of nanoscale three-branch junctions

J. Appl. Phys. **111**, 084511 (2012)

Additional information on J. Appl. Phys.

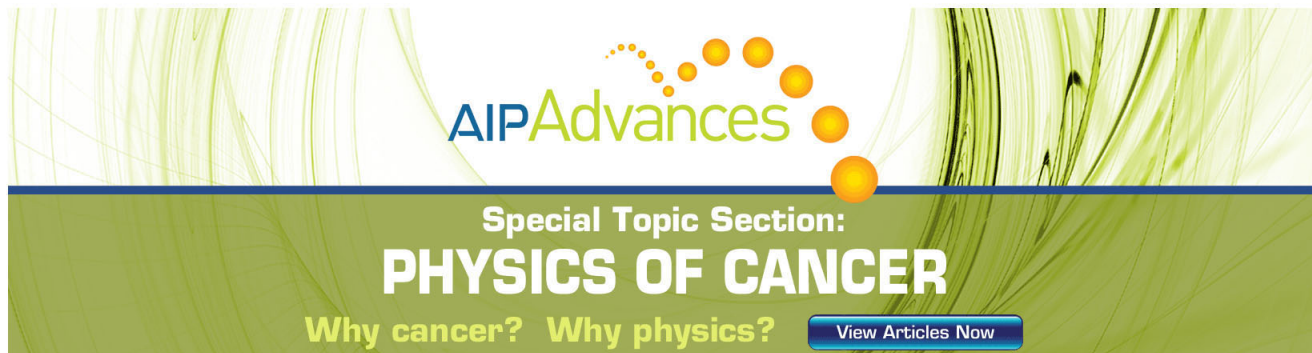
Journal Homepage: <http://jap.aip.org/>

Journal Information: http://jap.aip.org/about/about_the_journal

Top downloads: http://jap.aip.org/features/most_downloaded

Information for Authors: <http://jap.aip.org/authors>

ADVERTISEMENT



Special Topic Section:
PHYSICS OF CANCER

Why cancer? Why physics? [View Articles Now](#)

Engineering the strain field for the control of quantum confinement: An analytical model for arbitrary shape nanostructures

M. Mazzer^{a)}

Istituto Nuovi Materiali per l'Elettronica, Consiglio Nazionale delle Ricerche, via Arnesano, 173100 Lecce, Italy

M. De Giorgi and R. Cingolani

Istituto Nazionale per la Fisica della Materia (INFM), Dipartimento di Scienza dei Materiali—Università di Lecce, via Arnesano, 173100 Lecce, Italy

G. Porello, F. Rossi, and E. Molinari

Istituto Nazionale per la Fisica della Materia (INFM), Dipartimento di Fisica, Università di Modena, via Campi 213a, I41100 Modena, Italy

(Received 25 November 1997; accepted for publication 26 June 1998)

We describe an analytical method to calculate the strain field and the corresponding band gap modulation induced in a quantum well by a surface stressor of arbitrary shape. In this way, it is possible to engineer the confinement potential of different strained nanostructures based on patterned heterojunctions. Band gap modulations up to 130–140 meV are predicted for suitably designed II–VI/III–V and III–V/III–V heterostructures. © 1998 American Institute of Physics. [S0021-8979(98)02219-1]

I. INTRODUCTION

Low-dimensional structures have attracted interest for their optical and transport properties and for their applications to electrical and optoelectronic devices. The fabrication technology plays a crucial role in the determination of the desired quantization phenomena. So far, several ways of producing laterally confined structures in semiconductors have been proposed.¹ Most of them rely on material processing which induces sample damage, or on the difficult control of the self-organized growth.² An alternative technique for lateral quantum confinement is based on band gap modulation induced by strain gradients across a quantum well.³

The idea is to design and realize a proper pattern of free-standing stressors to generate a strain field whose intensity and modulation are such that lateral confinement is obtained in a quantum well a few nanometers below the surface. To engineer such a strain field, the shape, distribution, and dimension of the stressors must be determined according to the prediction of the elasticity theory. This optimization procedure is usually pursued numerically by using finite-element techniques⁴ which are quite accurate but require reiterated computations for any change of the structural parameters. The exact analytical solution of this elasticity problem is known only for very few and simple stressor shapes.⁵ In general, approximations are introduced by simplifying the boundary conditions or by using a series expansion method.

In this article, we show that accurate analytic solutions can be found when the amplitude of the relevant Fourier components of the surface profiles (the stressor patterns) are much smaller than the corresponding wavelengths. A method is presented which allows the solution of the elasticity problem for any surface profile, thus becoming extremely power-

ful and flexible for the design of new strain induced nanostructures.

II. MODEL

The pattern of stressors is treated as a thin film having a nonplanar surface, Σ , whose profile is described by the equation

$$y - tf(x, z) = 0, \quad (1)$$

where f is periodic function such that $-1 < f(x, z) < 1$ and t is the maximum amplitude of the profile modulation. The film is deposited on a semi-infinite ($y < 0$) planar substrate containing a quantum well at a given depth under the film-to-substrate interface. The problem is solved within the linear elasticity theory of an isotropic continuum.

If no body forces are present, an isotropic continuum satisfies the equilibrium equations and the compatibility conditions:

$$\begin{cases} (1 + \nu)\nabla^2 \boldsymbol{\sigma} + \tilde{\nabla} \nabla \text{Trace}(\boldsymbol{\sigma}) = 0, \\ \nabla \cdot \boldsymbol{\sigma} = 0, \end{cases} \quad (2)$$

where $\tilde{\nabla}$ is the transpose of the gradient vector ∇ , ν is the Poisson's ratio, and $\boldsymbol{\sigma}$ is the stress tensor, respectively.

The boundary conditions are given by the requirement that no net force acts upon the free surface, Σ , that is

$$0 = \boldsymbol{\sigma} \nabla [y - tf(x, z)] = \boldsymbol{\sigma} \hat{\mathbf{y}} - t \boldsymbol{\sigma} \nabla f, \quad (3)$$

where $\hat{\mathbf{y}}$ is the unit vector along the positive y direction.

If t is small compared to the period of the function f , along the two directions, it is reasonable to look for a solution of the elasticity equations [Eqs. (1) and (2)] having the form of a series expansion:

^{a)}Electronic mail: mazzer@osfime.unile.it

$$\boldsymbol{\sigma}(x, y, z) = \sum_{\alpha=0}^{\infty} t^{\alpha} \boldsymbol{\sigma}^{(\alpha)}(x, y, z). \tag{4}$$

For the same reason, the stress fields at the free surface [$y = tf(x, z)$] can be expanded in series around $y=0$, to obtain

$$\boldsymbol{\sigma}[x, tf(x, z), z] = \sum_{\beta=0}^{\infty} \sum_{\alpha=0}^{\infty} \frac{1}{\beta!} t^{\beta+\alpha} f(x, z)^{\beta} \left. \frac{\partial^{\beta} \boldsymbol{\sigma}^{(\alpha)}}{\partial y^{\beta}} \right|_{y=0}, \tag{5}$$

where the derivatives of the stress fields on the right hand side are calculated at $y=0$.

By using the series expansion in Eq. (5), Eq. (3) becomes

$$\sum_{\beta=0}^{\infty} \sum_{\alpha=0}^{\infty} \frac{1}{\beta!} t^{\beta+\alpha} f(x, z)^{\beta} \left. \frac{\partial^{\beta} \boldsymbol{\sigma}^{(\alpha)}}{\partial y^{\beta}} \right|_{y=0} \hat{\mathbf{y}} - \sum_{\beta=0}^{\infty} \sum_{\alpha=0}^{\infty} \frac{1}{\beta!} t^{\beta+\alpha+1} f(x, z)^{\beta} \left. \frac{\partial^{\beta} \boldsymbol{\sigma}^{(\alpha)}}{\partial y^{\beta}} \right|_{y=0} \nabla f = 0. \tag{6}$$

This is a power series which makes it possible to find the boundary conditions on the plane, $y=0$, at any order in t . Hence, by requiring that all the coefficients of the power series are zero a recursive formula is found which provides an explicit form for the boundary condition to be satisfied by the functions $\boldsymbol{\sigma}^{(\alpha)}(x, y, z)$.

At the zeroth order, Eq. (6) gives

$$\boldsymbol{\sigma}^{(0)}(x, 0, z) \hat{\mathbf{y}} = 0, \tag{7a}$$

which implies that the zeroth order stress is uniform in space, i.e., it is a constant tensor, $\boldsymbol{\sigma}^{(0)}$. Then, at the first order we get

$$\boldsymbol{\sigma}^{(1)}(x, 0, z) \hat{\mathbf{y}} = \boldsymbol{\sigma}^{(0)} \nabla f, \tag{7b}$$

and, finally, for $\alpha \geq 2$:

$$\begin{aligned} \boldsymbol{\sigma}^{(\alpha)}(x, 0, z) \hat{\mathbf{y}} &= \boldsymbol{\sigma}^{(\alpha-1)}(x, 0, z) \nabla f - \left[\sum_{\beta=1}^{\alpha-1} f(x, z)^{\beta} \left(\left. \frac{\partial^{\beta} \boldsymbol{\sigma}^{(\alpha-\beta)}}{\partial y^{\beta}} \right|_{y=0} \right) \hat{\mathbf{y}} \right. \\ &\quad \left. - \frac{1}{\beta!} \left. \frac{\partial^{\beta} \boldsymbol{\sigma}^{(\alpha-\beta-1)}}{\partial y^{\beta}} \right|_{y=0} \nabla f \right]. \end{aligned} \tag{7c}$$

The advantage of this method is that the boundary conditions now involve the stress on the plane, $y=0$. This makes it possible to search for a basic solution of the elasticity equations [Eq. (2)] having the form of a normal mode $\exp[i(nkx + mpz)]$ multiplied by a function of y . Then, thanks to the linearity of the boundary conditions [Eq. (7)], the general solution of the problem is found simply by using a Fourier expansion method.

A basic solution of Eq. (2) satisfying the requirement that the stress field tends to zero for y tending to $-\infty$ is uniquely given by

$$\begin{cases} \boldsymbol{\Psi}(x, y, z) = \exp[i(nkx + mpz) + Q_{nm}y](\mathbf{S} + y\mathbf{T}), \\ Q_{nm} = \sqrt{n^2k^2 + m^2p^2}, \end{cases} \tag{8}$$

where \mathbf{S} and \mathbf{T} are 3 by 3 matrices whose coefficients are independent of x , y , and z and depend linearly on three free parameters, c_1 , c_2 , and c_3 , to be determined by means of the boundary conditions at the surface, $y=0$. This gives the freedom to write the term $(\mathbf{S} + y\mathbf{T})$ as a linear combination of matrixes, $\mathbf{S}[j](n, m)$ and $\mathbf{T}[j](n, m)$ ($j = \{1, 2, 3\}$), such that

$$\begin{cases} \mathbf{S}[1](n, m) \hat{\mathbf{y}} = \hat{\mathbf{x}} \\ \mathbf{S}[2](n, m) \hat{\mathbf{y}} = \hat{\mathbf{y}} \\ \mathbf{S}[3](n, m) \hat{\mathbf{y}} = \hat{\mathbf{z}}. \end{cases} \tag{9}$$

With this choice, the forces acting upon the plane, $y=0$, have the simple form:

$$\begin{aligned} \boldsymbol{\Psi} \hat{\mathbf{y}}|_{y=0} &= \exp[i(nkx + mpz)](c_1, c_2, c_3) \\ &= \exp[i(nkx + mpz)] \mathbf{c}, \end{aligned} \tag{10}$$

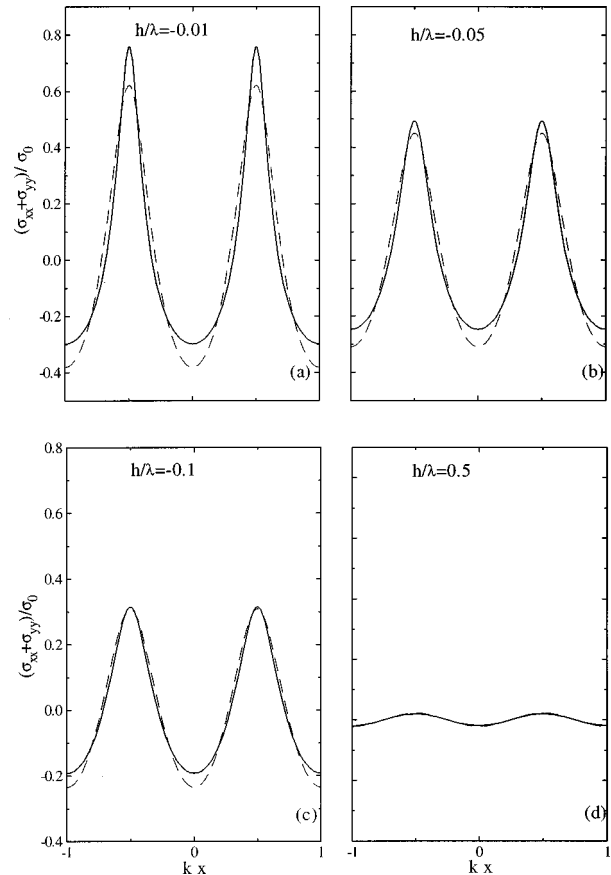


FIG. 1. Comparison between the stress field calculated exactly (solid line) and approximately (dashed line) at various distance ($-h$) from the interface for a rough surface which can be mathematically described by a cycloid with periodic cusps. The relation between width (t) and periodicity (λ) of the cycloid is $t/\lambda = 10\%$.

as it can be easily verified. The expression of the matrixes $\mathbf{S}[j](n,m)$ and $\mathbf{T}[j](n,m)$ are reported in the Appendix.

Now, the solution of the elastostatic problem [Eq. (2)], with boundary conditions given by Eq. (7), is straightforward. Consider a surface profile $f(x,z)$ which is periodic along \hat{x} and \hat{z} directions, the period being $2\pi/k$ and $2\pi/p$ respectively, and let $N_x k$ and $N_z p$ be the maximum wave vectors (multiples of the fundamentals k and p) in the Fourier expansion of the profile along the two directions.

The recursive formula for the boundary conditions [Eq. (7)] is such that the maximum wave vectors involved in the Fourier expansion of the right hand side of the equation is proportional to α . This gives, for $\alpha \geq 1$,

$$\sigma^{(\alpha)}(x,0,z)\hat{y} = \sum_{-\alpha N_x}^{\alpha N_x} \sum_{-\alpha N_z}^{\alpha N_z} m \mathbf{c}(n,m,\alpha) \exp[i(nkx + mpz)]. \tag{11}$$

Thanks to Eqs. (9) and (10), the solution of the elasticity problem at the order α is reduced to the calculation of the Fourier coefficients $\mathbf{c}(n,m,\alpha)$. In fact,

$$\sigma^{(\alpha)}(x,y,z) = \sum_{-\alpha N_x}^{\alpha N_x} \sum_{-\alpha N_z}^{\alpha N_z} \sum_{j=1}^3 c_j(n,m,\alpha) \{ \mathbf{S}[j](n,m) + y \mathbf{T}[j](n,m) \} \exp[i(nkx + mpz) + Q_{nm}y]. \tag{12}$$

In conclusion, the solution of the original elasticity problem is obtained recursively by calculating the Fourier transforms of the expression on the right hand side of Eq. (7) and by substituting the obtained coefficients into Eq. (12).

The calculation of the first-order solution is quite simple

for any surface profile. In fact Eq. (7b) shows that the solution is found simply by calculating the Fourier transform of the surface-profile gradient, ∇f .

Figure 1 shows the stress field calculated with our method and the one calculated exactly by Gao *et al.*⁵ for a surface profile which can be mathematically described by a cycloid. The comparison clearly shows that our calculation is quite accurate even at the first order approximation for a wide range of values of the amplitude to wavelength ratio. Moreover, our model can be used to evaluate the stress field for arbitrary stressor shapes and covers the vast majority of cases which have not been solved exactly so far.

III. RESULTS AND DISCUSSION

The most immediate application of our model is to determine how the electronic band structure in a quantum well, located a few nanometers below the free surface, can be properly tuned to introduce additional degrees of confinement for electrons and holes. In fact a lateral confinement potential is induced by the stressors in regions of the quantum well where compressive hydrostatic stress is released or where tensile hydrostatic stress is produced. Being analytical, the results of the calculation provide a straightforward recipe for the design of quantum wires and quantum dots having the desired electro-optical properties. In this section, our model is applied to the calculation of the hydrostatic stress induced by long rectangular stressors (giving rise to quantum wires) and square boxes (quantum dots).

For a periodic array of long stressors having a trapezoidal section, the major and minor bases being given by B and b , the first-order hydrostatic stress is given by $\sigma_{hy} = t\sigma_{hy}^{(1)} + \dots$, where t is the maximum thickness of the layer and

$$\sigma_{hy}^{(1)} = \frac{2(1+\nu)\sigma_0}{3\pi(B-b)} \log \left[\frac{\left(1 + e^{2ky} - 2e^{ky} \cos \left[\frac{k}{2}(B-2x) \right] \right) \left(1 + e^{2ky} - 2e^{ky} \cos \left[\frac{k}{2}(B+2x) \right] \right)}{\left(1 + e^{2ky} - 2e^{ky} \cos \left[\frac{k}{2}(b-2x) \right] \right) \left(1 + e^{2ky} - 2e^{ky} \cos \left[\frac{k}{2}(b+2x) \right] \right)} \right], \tag{13}$$

where ν is the Poisson ratio of the substrate, σ_0 is the misfit stress between the film and the substrate, and $k=2\pi/T$, T being the period of the stressor array. It is immediately seen that, for $y=0$, the first order hydrostatic stress exhibits singularities for $x = \pm B/2$ and $x = \pm b/2$, that is at the corners of the stressor. These singularities are an expected consequence of the presence of corners when the problem is solved within the linear elasticity theory. However, they are integrable, i.e., the displacement field is a continuous function, and they do not affect the shape and the magnitude of the stress field underneath the center of the stressor where the effect of strain confinement is studied.

In the case of a regular matrix of rectangular boxes, the first-order expansion of the hydrostatic component of the stress field is given by $\sigma_{hy} = t\sigma_{hy}^{(1)} + \dots$, where

$$\begin{aligned} \sigma_{hy}^{(1)} = & -\frac{\pi}{6} \sigma_0(1+\nu) \times \{ \chi_y(z) [\phi_y(-x,z) + \phi_y(x,z)] \\ & + \chi_y(-z) [\phi_y(-x,-z) + \phi_y(x,-z)] + \chi_y(x) \\ & \times [\phi_y(-z,x) + \phi_y(z,x)] + \chi_y(-x) \\ & \times [\phi_y(-z,-x) + \phi_y(z,-x)] \}, \end{aligned} \tag{14}$$

with

$$\begin{cases} \phi_y(u,\nu) = \frac{L_u + u}{\sqrt{(L_u + u)^2 + (L_\nu + \nu)^2 + y^2}}, \\ \chi_y(u) = \frac{L_u + u}{\sqrt{(L_u + u)^2 + y^2}}, \end{cases} \tag{15}$$

where L_x and L_z are the dimensions of the stressor box. As

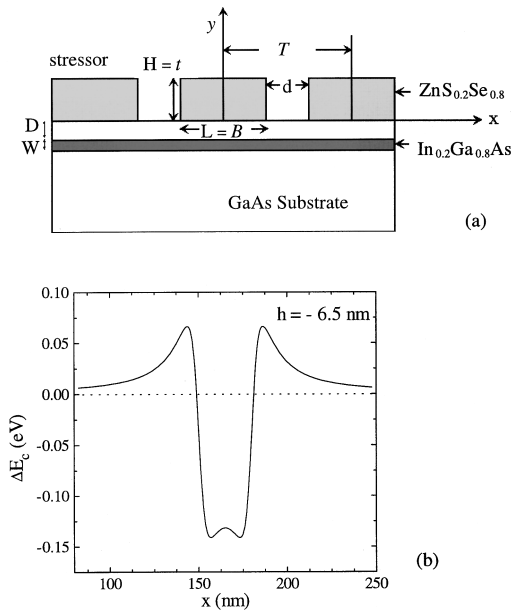


FIG. 2. (a) Schematic diagram of the stressed wire and substrate and (b) conduction band modulation at the center of QW.

in the previous case, this function exhibits singularities on the plane, $y=0$. It is easy to see that the stress diverges along the border of the box where, however, the displacement field is continuous. Finally, in the region occupied by the quantum well the stress is minimum just under the center of the stressor.

In general, the stress field modulation in the quantum well can be increased by increasing the aspect ratio of the stressor provided that the critical thickness for the generation of misfit dislocations is not exceeded.⁶

Our results show that, at the first order, the stress field decreases exponentially as the distance from the stressor increases. At the same time the stress gradient increases as the distance from the stressor decreases. This means that there is a trade off in choosing the most convenient location of the quantum well bearing in mind, also, that the well cannot be too close to the free surface to avoid image-charge effects.

In the following we report the results of the optimization procedure for two prototype low-dimensional structures. As a first example we discuss a heterostructure consisting of a $\text{In}_{0.2}\text{Ga}_{0.8}\text{As}/\text{GaAs}$ quantum well and barrier covered by $\text{ZnS}_{0.2}\text{Se}_{0.8}$ stressors. The thickness of the $\text{ZnS}_{0.2}\text{Se}_{0.8}$ layer, whose mismatch with respect to GaAs is +1.1%, is chosen in order to get the maximum strain modulation without ex-

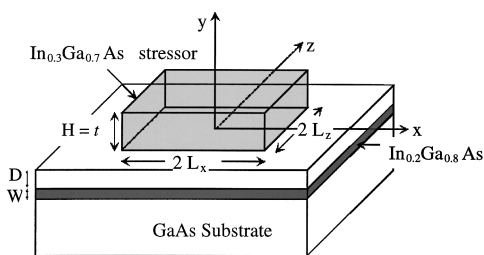


FIG. 3. Schematic diagram of the stressed dot and substrate.

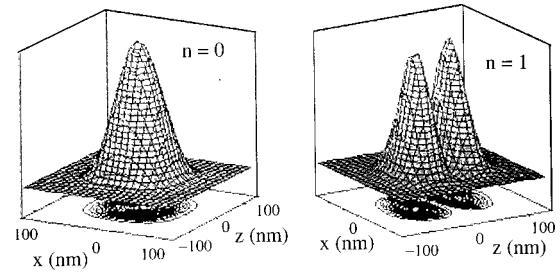


FIG. 4. Three-dimensional plot of the 0D electron density corresponding to the ground energy state ($n=0$) and the lowest excited level ($n=1$), which is degenerate in this structure.

ceeding the critical thickness for pseudomorphic growth (~ 40 nm). After the growth, the $\text{ZnS}_{0.2}\text{Se}_{0.8}$ layer is patterned to get 300-nm-wide stripes with 30 nm separation. The maximum band gap modulation is obtained for a 3-nm-wide quantum well buried below a GaAs barrier of 5 nm.

Since the strain in the $\text{ZnS}_{0.2}\text{Se}_{0.8}$ layer, before patterning, is uniformly tensile, lateral quantum confinement in the quantum well is obtained in the regions just below the voids between the stressors. The quantum well experiences a strain gradient resulting in a nearly parabolic lateral potential well (Fig. 2). The maximum modulation in conduction band $\Delta E_{c\text{Max}}$ is about 130 meV and the width of the lateral confining potential is approximately equal to the distance between stressors.

Another interesting example is shown in Fig. 3, where a quantum dot (QD) is obtained with a $\text{GaAs}/\text{In}_{0.2}\text{Ga}_{0.8}\text{As}$ quantum well stressed by $\text{In}_{0.3}\text{Ga}_{0.7}\text{As}$ square boxes. The thickness of the $\text{In}_{0.3}\text{Ga}_{0.7}\text{As}$ layer is 3 nm that is less than the critical thickness for pseudomorphic growth. The size of the $\text{In}_{0.3}\text{Ga}_{0.7}\text{As}$ stressors is $15 \times 15 \times 3 \text{ nm}^3$. In this case, the strain in the InGaAs layer, before processing, is uniformly compressive with a mismatch of -2.1% with respect to the GaAs substrate. This means that lateral confinement occurs just under the stressors rather than between them as in the case of tensile stress. In fact, the quantum well hydrostatic expansion due to the stressors has a maximum at the center of the square box, whereas it decreases towards the edges where a slight compression occurs.

This results in a box-shaped well for electrons. The maximum modulation in conduction band $\Delta E_{c\text{Max}}$ is now about 140 meV and the width of the well is approximately the same to the size of the stressors. For this structure, the single-particle energies and the associated eigenfunctions are calculated by solving numerically the Schrödinger equation in the envelope function approximation by means of a plane-wave expansion.⁷ Figure 4 shows a plot of the electron charge density corresponding to the first three electronic levels. The center of the stressor is located at $x=0$ and $z=0$. The ground state exhibits a single maximum at the center of the stressor, while the excited states exhibit an increasing number of maxima. It is evident that the electrons are confined laterally in the quantum well (QW). The energy splitting between the ground state and the first excited level is 40 meV which is larger than the thermal energy at room temperature.

IV. CONCLUSIONS

In summary, we have developed a new and simple method to calculate analytically the stress field induced in a quantum well by a stressor of arbitrary shape. The method allows one to engineer the strain distribution and the corresponding band gap modulation. Low-dimensional structures can easily be designed to get nearly parabolic lateral confining potentials with a band gap modulation as high as 130–140 meV and an interband splitting of about 40 meV. Due to its flexibility and simplicity this method is well suited for engineering a vast range of nanostructures, for instance by electron beam lithography, having the desired structural and electro-optical characteristics.

ACKNOWLEDGMENTS

This work has been partially supported by the ‘‘Progetto Sud: Quantum Wires V grooved for optoelectronic applications’’ of the INFM and by the EU-FESR subprogram 2.

APPENDIX

The explicit expression of the six matrixes appearing in Eq. (12) is the following:

$$\begin{aligned}
 \mathbf{S}[1] &= \begin{pmatrix} 0 & 1 & 0 \\ 1 & 0 & 0 \\ 0 & 0 & 0 \end{pmatrix} + \frac{i}{Q_{nm}^3} \\
 &\times \begin{pmatrix} 2nk(Q_{nm}^2 + vm^2p^2) & 0 & mp(Q_{nm}^2 - 2vn^2k^2) \\ 0 & 0 & 0 \\ mp(Q_{nm}^2 - 2vn^2k^2) & 0 & 2vn^3k^3 \end{pmatrix}, \\
 \mathbf{S}[2] &= \begin{pmatrix} 1 & 0 & 0 \\ 0 & 1 & 0 \\ 0 & 0 & 1 \end{pmatrix} + \frac{(1-2\nu)}{Q_{nm}^{(2)}} \begin{pmatrix} m^2p^2 & 0 & mpnk \\ 0 & 0 & 0 \\ mpnk & 0 & n^2k^2 \end{pmatrix},
 \end{aligned}$$

$$\begin{aligned}
 \mathbf{S}[3] &= \begin{pmatrix} 0 & 0 & 0 \\ 0 & 0 & 1 \\ 0 & 1 & 0 \end{pmatrix} + \frac{i}{Q_{nm}^3} \\
 &\times \begin{pmatrix} 2vm^3p^3 & 0 & nk(Q_{nm}^2 - 2vm^2p^2) \\ 0 & 0 & 0 \\ nk(Q_{nm}^2 - 2vm^2p^2) & 0 & 2mp(Q_{nm}^2 + vn^2k^2) \end{pmatrix},
 \end{aligned}$$

$$\mathbf{T}[1] = \frac{ink}{Q_{nm}} \mathbf{T}[2],$$

$$\mathbf{T}[2] = \begin{pmatrix} \frac{n^2k^2}{Q_{nm}} & -ink & \frac{nkmp}{Q_{nm}} \\ -ink & -Q_{nm} & -imp \\ \frac{nkmp}{Q_{nm}} & -imp & \frac{m^2p^2}{Q_{nm}} \end{pmatrix},$$

$$\mathbf{T}[3] = \frac{imp}{Q_{nm}} \mathbf{T}[2].$$

The determinant of $\mathbf{T}[2]$ is equal to zero and it is easy to see that $\mathbf{T}[2]^2 = 0$.

- ¹R. Cingolani and R. Rinaldi, Riv. Nuovo Cimento **16**, (1993).
- ²M. Sapanen, H. Lipsanen, and J. Ahopelto, Appl. Phys. Lett. **66**, 2364 (1995).
- ³K. Kash, J. M. Worlock, M. D. Sturge, P. Grappe, J. P. Harbison, A. Scherer, and P. S. D. Lin, Appl. Phys. Lett. **53**, 782 (1988).
- ⁴K. Kash, R. Bhat, D. D. Mahoney, P. S. D. Lin, A. Scherer, J. M. Worlock, B. P. Van der Gaag, M. Koza, and P. Grappe, Appl. Phys. Lett. **55**, 681 (1989).
- ⁵C. H. Chiu and H. J. Gao, Int. J. Solids Struct. **30**, 2983 (1993).
- ⁶J. W. Matthews and A. E. Blakeslee, J. Cryst. Growth **27**, 118 (1974).
- ⁷R. Rinaldi *et al.*, Phys. Rev. Lett. **73**, 2899 (1994).